Australian Journal of Basic and Applied Sciences, 4(8): 3077-3085, 2010
ISSN 1991-8178

A comparative Analysis of Experimental and Numerical Investigations of Composite Tubes under Axial and Lateral Loading

[1]Hakim S. Sultan Aljibori, [1]Haidar F. Al-Qrimli, [1]Rahizar Ramli, [2]E. Mahdi, [3]Faris Tarlochan and [1]Chong W. P

[1]Department of Mechanical Engineering, University of Malaya, 50603 Kuala Lumpur, Malaysia
[2]Department of Mechanical and industrial Engineering, Qatar University, Qatar
[3]College of Engineering, Universiti Tenaga Nasional, 43009 Kajang, Selangor, Malaysia

Abstract: Quasi-static tests are performed in order to determine the crash behavior of composite tubes. The specimens are made from woven fiber carbon/epoxy. The crash experiments show that the tubes crushed in a progressive manner from one end to the other of the tubes while delamination was - taking place between the layers. In the simulation works described in this paper the ANSYS explicit finite element code is used to investigate the compressive properties and crushing response of circular carbon tube subjected to static axial and lateral loading and the results are compared with the experimental work. To better understand the details of the crash process, thin multi layer shell elements are used to model the walls of the circular tube. Finally, the design optimization technique is implemented to find an optimum composite configuration that has the maximum failure load and absorbs the most energy. The crash performance of a carbon composite shell is compared with an optimum carbon tube from the experimental work.

Key words: Composites, Circular tubes, Axial compression, Lateral compression and Finite element simulation.

INTRODUCTION

Great records of articles have considered the crash performance of thin tube structures made from conventional metal as well as fiber reinforced composite. In automotive applications, crashworthy structures absorb impact energy in a controlled manner, thereby bringing the passenger compartment to rest without subjecting the occupant to high deceleration. A typical characteristic of such a deformation mechanism is that the rate of energy dissipation is concentrated over relatively narrow zones, while the remainder of the structure maintains its rigidity. In comparison to metals, most composites generally collapse in a brittle manner, failing through a sequence of fracture mechanisms involving fiber fracture, matrix crazing and cracking, fiber-matrix debonding, delamination and internal ply separation (Ramakrishna, 1997). The preface of composite materials in vehicles not only increases the energy absorption per unit of weight but also the noise and vibrations are reduced, in comparison with structures made from steel or aluminum (Shin *et al.,* 2002; Zarei and Kro ger, 2006, Feillard, 1999).

The important crashworthiness parameters are the total energy absorption (TEA) and specific energy absorption (SEA) capabilities. The total energy absorption is equal to the area under the crash load–displacement curve while specific energy absorption is defined as the energy absorption per crushed mass. In one of the studies (Hamada and Ramakrishna, 1997), axi-symmetric carbon Poly-Ether-Ether-Ketone (PEEK) composite tubes were tested quasi-statically and dynamically with progressive crushing initiated at a chamfered end. The tubes underwent quasi static crushing, and displayed high specific energy absorption as a result of different crushing mechanisms attributed to different crushing speeds. The quasi-static- tested tube splayed into well-defined fronds, while the impact tested tube walls were crushed by brittle fracture. Mamalis *et al.* (1997;2005) investigated the crash behavior of square composite tubes subjected to static and dynamic axial compression. They observed a stable progressive collapse mode coupled with high amounts of energy absorbed and a mid-length collapse mode characterized by brittle and catastrophic failure in their experiments. The load–displacement curve for the static testing exhibited classic peaks and valleys with a slight fluctuation in

Corresponding Author: Hakim S. Sultan Aljibori, Department of Mechanical Engineering, University of Malaya, 50603 Kuala Lumpur, Malaysia
Email: hakimss@um.edu.my Tel: ++603 7967622 Fax: ++603-79675317

amplitude. Soon after, Mamalis *et al.* (2006) investigated the crashing uniqueness of thin walled, carbon fiber reinforced plastic tubular mechanism. They made a comparison between the quasi static and dynamic energy absorption ability.

The high cost of the experimental and physical testing makes design validation by means of numerical methods very attractive. Mamalis *et al.* (2006) and Bisagni *et al.* (2005) used the explicit finite element code, LS-DYNA, to simulate the crash reaction of composite tubes. They used their experimental results to confirm the simulations. El-Hagel *et al.* (2004) used the finite element method to study the quasi-static axial crush behavior of an aluminum composite hybrid tube containing filament wound E glass fiber reinforced epoxy over-wrap around an aluminum tube. The fiber orientation angle in the over-wrap was ±45 to the tube axis.

Dynamic crash tests were performed by Hamidreza *et al.* (2008) who fabricated specimens made from woven roving fiber. Their investigations deal with the experimental and numerical crashworthiness of square composite tubes. Thin shell elements were used to model the tube walls. The contact between the tube walls during deformation used a surface-to-surface contact algorithm to model the glue on the walls. (Gupta and Nagesh, 2006) studied the transition of deformation mode shapes of round aluminum tubes. Quasi-static axial experiments were carried out on aluminum tubes and compared with numerical simulation. The numerical simulation of the collapse was undertaken using a static non-linear finite element analysis in ANSYS software. They used a 20-node quadratic 3D brick element with 2 elements in thickness direction and surface-to-surface contact and found that the folding pattern in FE simulation occurs at the end of the tube in contrast with experiments where it occurs at the top of the tube. (Nagel and Thambiratnam, 2004) studied the energy absorption response of straight and tapered thin-walled rectangular tubes under both quasi-static and dynamic axial impact loading, for variations in wall thickness and-, taper angle. They set up that the dynamic reaction of tapered tubes is more sensitive to impact velocity and wall thickness than taper angle for lower impact velocities. Surface-to-surface algorithm contact between each rigid surface and the tube was used. The shell surface contact in the FE model was treated as frictionless. Mahdi *et al.* (2006) found that throughout the simulation process, as the number of corrugations increases, the amount of absorbed energy significantly increases. Three different tube geometries were modeled by Spagnoli *et al.* (2001); straight tubes, corrugated tubes with different corrugation angles, and tubes with higher number of corrugation surfaces. Shell elements are used in their model structure.

Present numerical models have been used to study the buckling behavior of laminated woven cylinders subjected to axial compression, and non-linear simulations have been undertaken to study the behavior of the composite cylinders. Although several published studies have been conducted to determine the crash characteristics of composite tubes, only few attempts have been made to optimize those behaviors.

Experimental Setup:

Axial and lateral loads have been applied on a carbon fiber specimen with circular geometry and a ±45 fiber orientation angle. The wall thicknesses of the tube was 2.7 mm with a length of 100 mm as shown in Figure 1, with the hand-lay-up method being used to fabricate the specimens as shown in Figure 2.

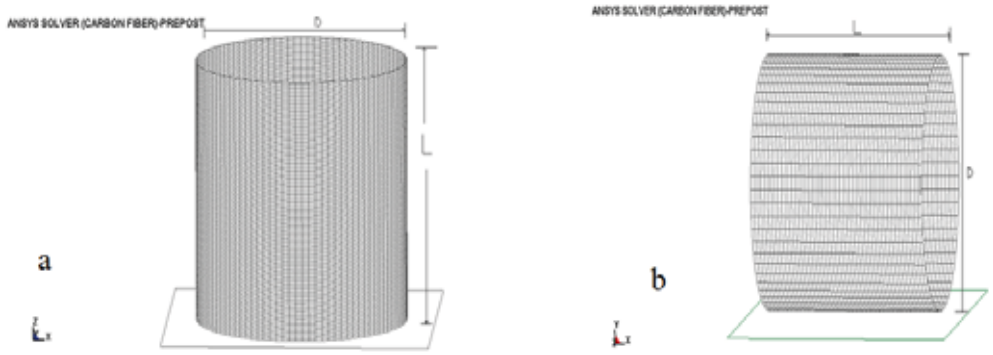

Fig. 1: Mesh generation of (a) the axial loading test and (b) the lateral loading test.

The tube is fabricated by rolling the woven roving carbon onto a rotating wooden mandrel of a circular section. The woven roving carbon fiber is passed through a resin bath by using a brush to make sure the

specimens have equal amounts of epoxy/resin. The fabricated tube is cured at room temperature (26 C) and left for 24 hrs to provide optimum curing. Finally the cured tube is extracted from the mandrel and cut into the desired dimensions needed for the physical test. A special designed mandrel is used for fabrication of the specimens. Epoxy/resin is used as the matrix of the composite structure. One hundred 100 ml of resin was mixed carefully with 20 ml of hardener. An electrical mixture is used to give an excellent mixing process. The fabrication process was carried out under identical conditions with a fixed fiber orientation of ±45° and the same geometry. The specimens are tested in quasi-static axial compression between two flat steel plates one of which is static and the other one moving at a constant speed of 15 mm/min by using the - INSTRON 4469 digital testing machine with full scale load range of 100kN (Fig.3). Three specimens for each composite tube type are tested. Load and displacement were recorded by an automatic data acquirement system.

Fig. 2: Hand lay-up Experimental work

Fig. 3: INSTRON machine

Finite Element Modeling

ANSYS is a very powerful and impressive computational tool that is used to solve many engineering problems. When performing the dynamic analysis of a structure, the most important concern of the analyst is to find out how the structure will respond over time to a given set of conditions (loads, motion, impact with another structure, etc.). The required input data can be classified into the following categories:

Model Development:

The ANSYS model is a graphical representation consisting of geometric features (pointes, lines, surfaces, and volumes) and assigned attributes (mesh, geometry, materials, loading, and supports). The finite element simulation described here is done in three steps, the first one being the building of the model as shown in Figure 1, the second step being the non-linear dynamic analysis and the final one being the post-processing of the results. The shell length and inner diameter were constant at 100 mm and 100 mm, respectively. The test was designed and implemented allowing the rigid solid steel plate to move and push into the composite shell as shown in Figure 4 (axial) and Figure 5 (lateral).

Material Properties:

The composite material properties used in this study can be summarized as shown in Table 1.

Table 1: Material Properties

Material Property	Symbol	Property Value
Mass Density	ρ	1.8 g/cm3
Young's modulus - longitudinal direction	Ea	3.2 GPa
Young's modulus - transverse direction	Eb	4.199 GPa
Young's modulus - normal direction	Ec	8.199 GPa
Poisson's ratio ba	PRBA	0.35
Poisson's ratio ca	PRCA	0.35
Poisson's ratio cb	PRCB	0.3
Shear Stress	Gab	4.00 GPa
Shear Stress	Gbc	4.00 GPa
Shear Stress	Gca	3.98 GPa
Material angle	BETA	45°

Boundary Condition:

The boundary conditions of the composite tube are that one end was loaded by a rigid steel plate, while the other end was fully constrained in all degrees of freedom (DOF). The total duration of the analysis was set at 6 seconds.

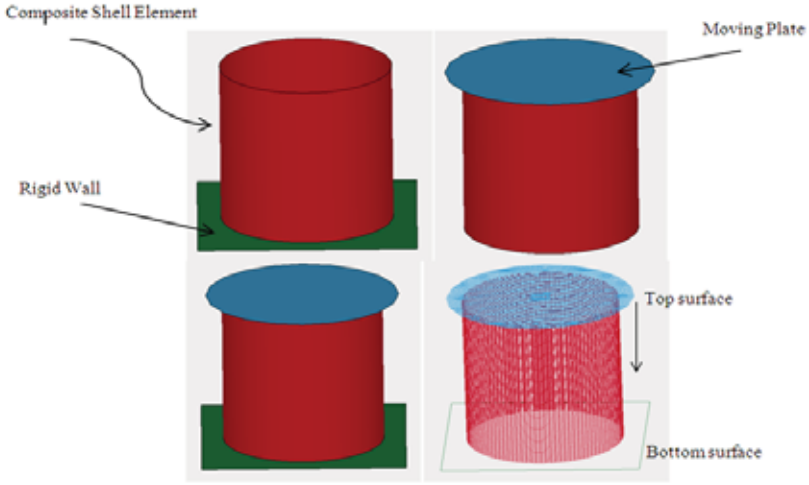

Fig. 4: Boundary Conditions of FEA Axial Test

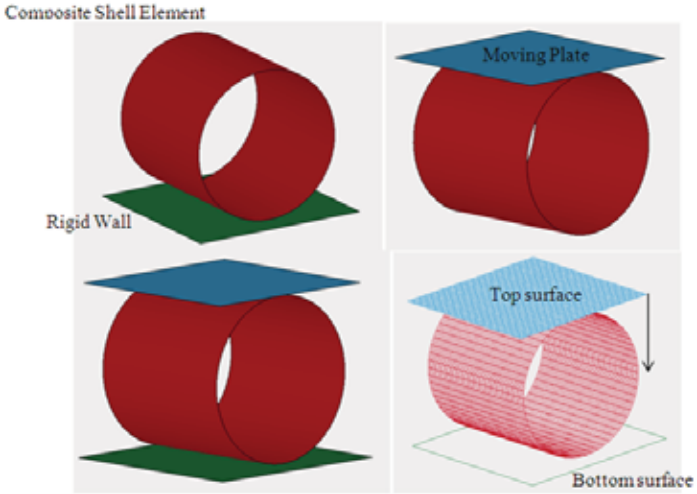

Fig. 5: Boundary Conditions of FEA lateral Test

Contact:

Equally important as the geometry, meshing, type of element and material properties, are the contact definitions for interacting parts of the model Contact elements and automatic surface-to-surface (ASTS) contact is used during the crushing between the steel plate and the composite shell.

Experimental and Numerical Results:

The individual ability to withstand shock loading depends on the period and deceleration of the crash pulse. Thus, the crush time is one of the most important parameters to characterize the vehicle occupant damage. The crushing sequence of the axial loading and the different types of failures are shown in Figure 6. When time T= 0sec there is no deflection in the model but when the time reaches 0.599 sec it starts splaying to the outside of the tube which is progressive failure mode as shown in Figure 7. While the time is running complex failure modes occur in the model between buckling and folding. The buckling of the model starts when the time is equal to 2.6 sec while the delamination cracks are clear at T= 3.5sec. At T= 6.00 sec the test ends and the folding failure mode is clear at this stage. The lateral loading test (Figure 8) starts when the time is equal to zero second and ends at 4.5 sec. The failure becomes clear when T= 1.5sec and continues until the end as shown in Figure 9.

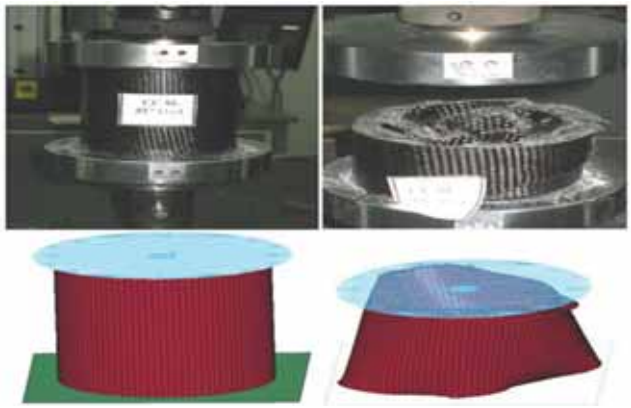

Fig. 6: Experimental and FEA Axial Test

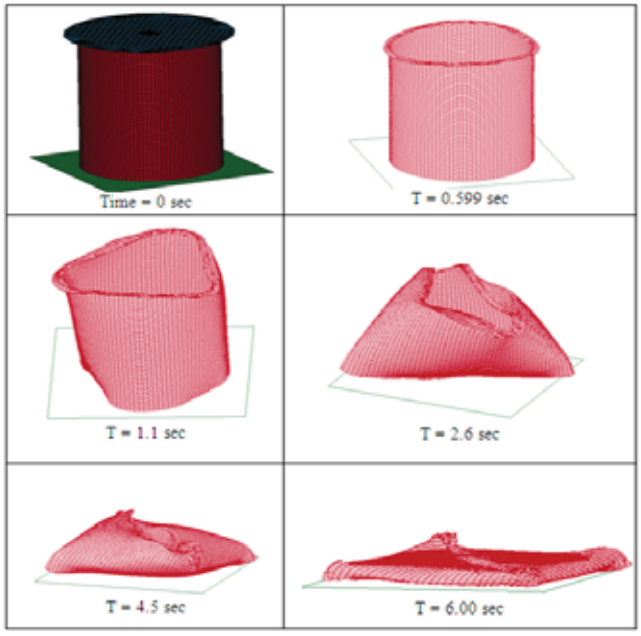

Fig. 7: Time Steps of the axial crushing

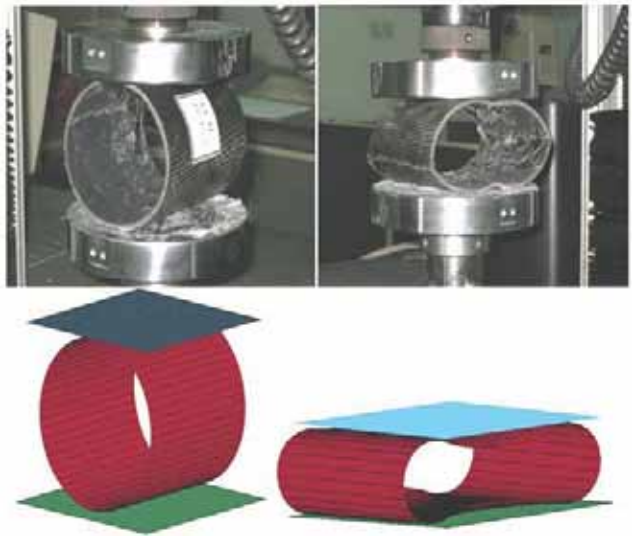

Fig. 8: Experimental and FEA Lateral Test

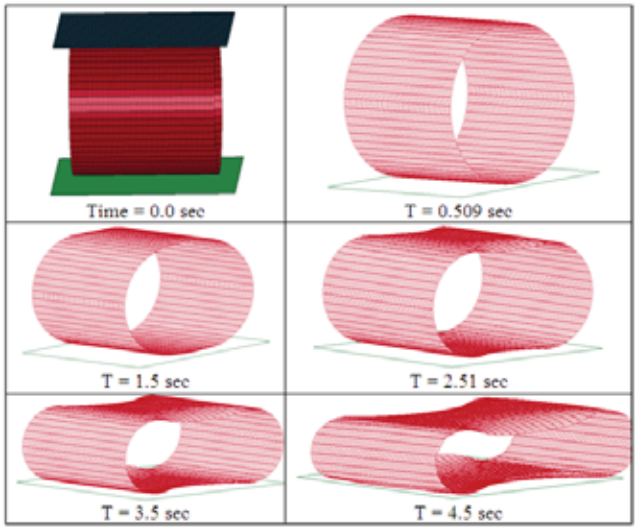

Fig. 9: Time Steps of the lateral crushing

Comparison between Experimental Results and Finite Element Analysis:

Figures 10 and 11 show that the load-displacement curves of the experimental results obtained from this study have been compared with finite element results by using ANSYS/LS DYNA software for axial and lateral loading. The maximum failure load and the average crushing load are discussed and the calculations of the crashworthiness parameters are listed in Table 2. The load- displacement curves of the experimental and the finite element are shown to draw comparisons. It is clear that the curves have the same trend. The maximum failure load for the FEA (P_{max}= 52.81kN) produced a higher value in comparison to the experimental results (P_{max}= 48.16kN). According to the crashworthiness parameters it was calculated that the FEA results produced more energy absorption than the experimental results, but the load ratio is the same for both the experimental and FEA results because the initial failure load is equal to the maximum failure load. In the lateral loading test the experimental results produced a higher value for maximum failure load with (P_{max}= 3.00kN) compared with FEA (P_{max}= 2.88kN). In addition the slop of the FEA has the same path as the experimental curve because in the experiment there are two types of failure modes which occur. In both of the specimens the finite element and experimental buckling failure mode occur, but in the experimental results

fiber breakage can be seen when the load reaches the peak, with a sharp drop occurring in the load curve because of the fiber breakage. The difference is clear. The total energy absorption (TEA) and the crush force efficiency of experimental results have higher values. Table 3 shows the crashworthiness parameters of the experimental and FEA results.

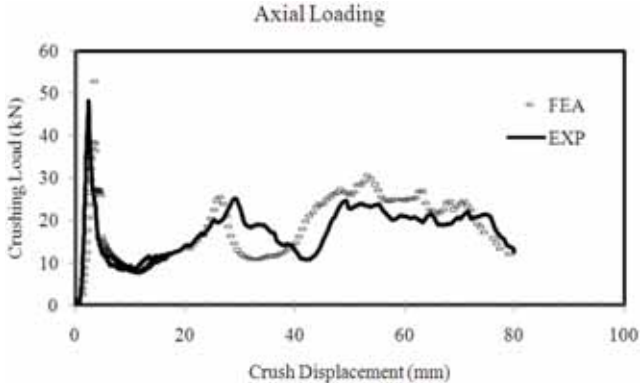

Fig. 10: Load-displacement curve of experimental and FEA (Axial loading).

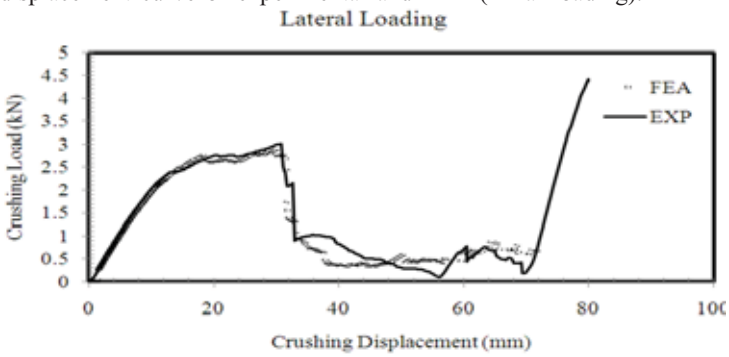

Fig. 11: Load-displacement curve of experimental and FEA (Lateral loading).

Table 2: Compression between FEA and the experimental work

Test type	FEA		EXP	
Load (kN)	P_{max}	P_{av}	P_{max}	P_{av}
Axial loading	52.81	16.01	48.16	15.41
Lateral loading	2.88	1.29	3.00	1.47

Table 3: Crashworthiness parameters of experimental and FEA results

Test type		PR kN/kN	TEA kJ	SEA kJ/Kg	VEA kJ/m3	CFE kJ	C mm/mm
Axial	FEA	1	3.99	43.48	50.87	0.3	0.75
loading	EXP	1	3.73	40.65	47.56	0.31	0.77
Lateral	FEA	1	0.11	1.3	1.52	0.44	0.41
loading	EXP	0.79	0.16	1.74	2.03	0.48	0.66

Stress:

The stress which occurred on the carbon shell has been discussed. From Figures 12 and 13, the blue color refers to the steady state, which means there is no stress on the tube. Moving the plate down will cause a stress along the shell and the centre of this maximum stress is in the middle of the tube which is represented in red. While the plate moves down, three red spots of stress will appear on the surface of the tube. The beginning of the buckling transfers the three spots of the maximum stress into two spots with the proceeding of the plate. Reaching 80 mm which is the end point of the crash distance the area of the stress becomes smaller. From all of the above, we can conclude that the stress was allocated mostly in the middle of the shell. Surprisingly, the lateral loading test shows us that the centre of the maximum stress is occurred in the middle of the tube as well.

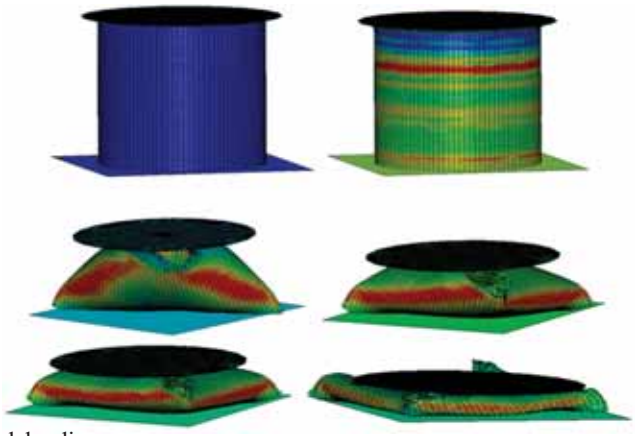

Fig. 12: Stresses in axial loading.

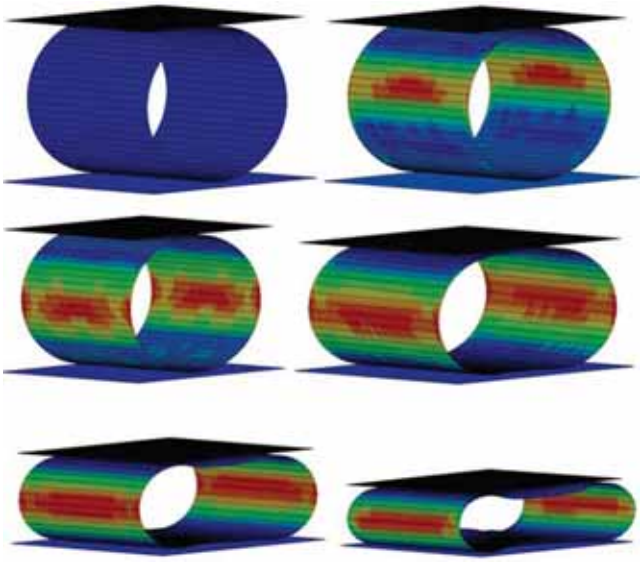

Fig. 13: Stresses in lateral loading

Failure Modes:

When a solid steel plate moves during the composite shell, the fibers directly below the plate provide the resistive force to the steel plate motion. This resistance and force are exerted by the composite and, at the same time the carbon shell is deformed during the crush and the initial deformation of the shell takes place by increases in radial direction and the damage developed from the moving of plate at the one edge of the carbon shell. These deformations in the composite structure cause some energy absorption. The specimen shows that the failure occurs in the contact area between the solid steel plate and composite carbon shell. These failure modes may be summarized as:

1. Matrix cracks lead to the splitting of the inner most wall layer of the composite shell.
2. With the continuous slipping of the solid plate and growth of damage, the innermost layer experiences

Conclusion:

In the experimental part we could not know exactly the particular value for several factors for instance time, stress, and failures. Using the finite element simulation helped us to better understand these three measurements. Comparison between the experimental and finite element results is made. Furthermore, this comparison was carried out to observe the effect of combined axial and lateral loads on the crushing of the composite tube which emerged as the optimum shape in the experimental work. Carbon fiber reinforced composite tube, using a matrix of epoxy resin and hardener, was fabricated. The tube has a ±45° orientation

angle, 100 mm length and 2.70 mm tube thickness. It has been seen that the tendency of the curves is almost the same between the experimental and the finite element results.

ACKNOWLEDGMENTS

The authors would like to thank University of Malaya for their financial support for this research.

Nomenclature

CG	Circular Carbon Fiber
P_i	Initial Failure Load
P_{max}	Maximum Failure Load
P_{av}	Average Failure Load
D_i	Initial Displacement
D_f	Final Displacement
PR	Load Ratio
TEA	Total Energy Absorption
SEA	Specific Energy Absorption
VEA	Volumetric Energy Absorption
CFE	Crush Force Efficiency
C	Crush Strain Relation

REFERENCES

Bisagni, C., G.D. Pietro, L. Fraschini and D. Terletti, 2005. Progressive crushing of fiber-reinforced composite structural component of a formula one racing car. Compos Struct., 68: 491–503.

El-Hagel, H., P.K. Mallick and N. Zamani, 2004. Numerical modeling of quasistatic axial crash of square aluminum-composite hybrid tubes. Int J Crashworthiness., 9(6): 653–64.

Feillard, P., 1999. Crash modeling of automotive structural parts made of composite materials. In: Proceedings of the SAE international congress and exposition, Detroit, MI, pp: 1–4.

Gupta, N.K. and Nagesh, 2006. Collapse mode transitions of thin tubes with wall thickness, end condition and shape eccentricity. Department of Applied Mechanics, Indian Institute of Technology, Delhi 110016, India, International Journal of Mechanical Sciences., 48: 210–223.

Hamada, H. and S.A. Ramakrishna, 1997. FEM method for prediction of energy absorption capability of crashworthy polymer composite materials, Journal of Reinforced Plastic Composite, 16(3): 226–42.

Hamidreza Zarei, Kro¨ger Matthias, Henrik Albertsen, 2008. An Experimental and Numerical Crashworthiness Investigation of Thermoplastic Composite Crash Boxes. Institute of Dynamics and Vibrations, 30167 Hannover, Germany Composite Structures., 85: 245–257.

Mamalis, A.G., D.E. Manolakos and G.A. Demosthenous, M.B. Ioannidis, 1997. The static and dynamic axial crumbling of thin-walled fiberglass composite square tubes. Composites Part B., 28B(4): 439–51.

Mamalis, A.G., D.E. Manolakos, M.B. Ioannidis and D.P. Papapostolou, 2005. On the response of thin-walled composite tubular components subjected to static and dynamic axial compressive loading: Experimental. Compos Struct., 69: 407–20.

Mamalis, A.G., D.E. Manolakos, M.B. Ioannidis and D.P. Papapostolou, 2006. The static and dynamic axial collapse of CFRP square tubes: finite element modeling. Compos Struct., 74: 2213–50.

Mahdi, E., A.S. Mokhtar, N.A. Asari, F. Elfaki, E.J. Abdullah, 2006. Nonlinear Finite Element Analysis of Axially Crushed Cotton Fiber Composite Corrugated Tubes, Composite Structures., 75: 39–48.

Nagel, G.M. and D.P. Thambiratnam, 2004. A Numerical Study on the Impact Response and Energy Absorption of Tapered Thin-Walled Tubes. International Journal of Mechanical Sciences, 46: 201–216.

Ramakrishna, S., 1997. Micro structural design of composite materials for crashworthy applications. Mater Des., 18: 167–73.

Shin, K.C., J.J. Lee, K.H. Kim, M.C. Song and J.S. Huh, 2002. Axial crash and bending collapse of an aluminum/GFRP hybrid square tube and its energy absorption capability. Compos Struct., 57: 279–87.

Spagnoli, A., A.Y. Elghazouli, M.K. Chryssanthopoulos, 2001. Numerical simulation of glass-reinforced plastic cylinders under axial compression. Marine Structures., 14: 353-374.

Zarei, H.R. and M. Kro¨ger, 2006. Multiobjective crashworthiness optimization of circular aluminum tubes. Thin-Walled Struct J 44: 301–8.